

# Experimental generation of pseudo bound entanglement

Hermann Kampermann\* and Dagmar Bruß

*Institut für Theoretische Physik III, Heinrich-Heine-Universität Düsseldorf, D-40225 Düsseldorf, Germany*

Xinhua Peng

*Experimentelle Physik IIIa, Technische Universität Dortmund, D-44221 Dortmund, Germany and  
Hefei National Laboratory for Physical Sciences at Microscale and Department of Modern Physics,  
University of Science and Technology of China, Hefei, Anhui 230026, People's Republic of China*

Dieter Suter

*Experimentelle Physik IIIa, Technische Universität Dortmund, D-44221 Dortmund, Germany*

(Dated: September 15, 2009)

We use Nuclear Magnetic Resonance (NMR) to experimentally generate a bound entangled (more precisely: pseudo bound entangled) state, i.e. a quantum state which is non-distillable but nevertheless entangled. Our quantum system consists of three qubits. We characterize the produced state via state tomography to show that the created state has a positive partial transposition with respect to any bipartite splitting, and we use a witness operator to prove its entanglement.

PACS numbers:

Quantum entanglement has been a source for fascination and surprise for more than 70 years [1]. The discovery that entanglement can serve as a resource for information processing has triggered the development of the broad field of quantum information science [2, 3]. Designing and controlling entangled quantum states has thus become a major experimental challenge. Several types of entangled states have already been experimentally generated and detected in the recent years, e.g. bipartite entanglement [6, 7], tripartite entanglement [8, 9, 10], as well as multipartite entanglement [11, 12, 13, 14].

A particularly interesting class of entangled states are “bound entangled” states [15], which carry quantum correlations of an especially elusive and fragile type. The name “bound entanglement” implies an analogy to bound energy in thermodynamics, which cannot be freed to perform work. Bound entanglement can be described as inherent quantum correlations, without the typical information processing potential of “free” entanglement. Namely, some correlations of quantum nature are initially established during the generation of a bound entangled state, but nevertheless it is not possible to extract a maximally entangled state for any number of copies of the state (i.e., entanglement distillation is not possible for bound entangled states). However, it has been shown that under certain circumstances bound entanglement can nevertheless be useful to establish a secret key [16]. Bound entanglement is expected to exist in Nature - for example it was shown theoretically in [17] that thermal states of several spin models carry bound entanglement. Bound entangled states are always mixed, and due to the small region that they occupy in the space of all states, they are vulnerable to decoherence. There-

fore, it is challenging to create and detect them in the laboratory.

Here, we report on the first experiment in which pseudo bound entanglement is created and observed [18]. We generate a bound entangled state of a class initially suggested by Acin *et al.* [19] with Nuclear Magnetic Resonance (NMR), and show their undistillability via state tomography, by proving that the partial transposes are positive. A suitable entanglement witness is implemented to detect the entanglement [20]. As usual in room temperature NMR we work with states close to the (normalised) identity, i.e. we consider a state of the form

$$\rho = \frac{1-p}{d} \mathbb{1} + p\rho_{BE}, \quad (1)$$

where  $\rho_{BE}$  is the bound entangled density matrix. We therefore call the whole state  $\rho$  pseudo bound entangled. This is in analogy with the NMR GHZ state [21]. NMR technology has been widely used to demonstrate quantum information primitives [22, 23, 24, 25, 26], and here it proves again to be a versatile tool.

We consider the family of three-qubit states defined in [19]:

$$\begin{aligned} \rho_{BE} = N^{-1} & \left( 2|\text{GHZ}\rangle\langle\text{GHZ}| + \right. \\ & a_1|001\rangle\langle001| + a_2|010\rangle\langle010| + \frac{1}{a_3}|011\rangle\langle011| + \\ & \left. a_3|100\rangle\langle100| + \frac{1}{a_2}|101\rangle\langle101| + \frac{1}{a_1}|110\rangle\langle110| \right), \end{aligned} \quad (2)$$

where  $|\text{GHZ}\rangle = \frac{1}{\sqrt{2}}(|000\rangle + |111\rangle)$ , and the normalisation is  $N = \left( 2 + \sum_{i=1}^3 (a_i + \frac{1}{a_i}) \right)$ . The free parameters  $a_1, a_2, a_3$  are real positive numbers that obey the condition  $a_1 a_2 a_3 \neq 1$ . This family of states is “almost” diagonal, with the only off-diagonal matrix elements coming

---

\*Electronic address: kampermann@thphy.uni-duesseldorf.de

from the GHZ contribution, see Fig. 2 for a visual representation. The states have rank 7 and are thus far from being pure. The states in equation (2) have a positive partial transposition (PPT) with respect to any bipartite splitting, but it was shown that they are nevertheless entangled [19]. Therefore, they are bound entangled.

In [20] a family of witness operators which detects the bound entangled states in equation (2) was presented. The family of witnesses has the form

$$W = \overline{W} - \varepsilon \mathbb{1} \quad (3)$$

with

$$\begin{aligned} \overline{W} = & |GHZ^-\rangle\langle GHZ^-| \\ & + \frac{1}{1+a_1^2} \left( |001\rangle\langle 001| + a_1^2 |110\rangle\langle 110| \right) \\ & + \frac{1}{1+a_2^2} \left( |010\rangle\langle 010| + a_2^2 |101\rangle\langle 101| \right) \\ & + \frac{1}{1+a_3^2} \left( |100\rangle\langle 100| + a_3^2 |011\rangle\langle 011| \right) \\ & - \sum_{i=1}^3 \frac{a_i}{1+a_i^2} \left( |000\rangle\langle 111| + |111\rangle\langle 000| \right). \end{aligned} \quad (4)$$

where  $|GHZ^-\rangle = \frac{1}{\sqrt{2}}(|000\rangle - |111\rangle)$ . Note that we are not using any specific normalisation of the witness. We choose the set of free parameters for the state and witness in such a way that the witness detects entanglement with the highest fraction of white noise. The optimal parameters calculated via convex optimization are  $a_1 = a_2 = a_3 = a = 0.3460$  and  $\varepsilon = 0.1069$  [20].

A perfect experimental realisation of the bound entangled state  $\rho_{BE}$  would lead to the expectation value  $\text{tr}(W\rho_{BE}) = -\varepsilon$ . This is obvious by construction, as  $\overline{W}$  is decomposable (i.e. it can be written as the sum of a positive operator and the partial transpose of another positive operator), and therefore its expectation value for a PPT bound entangled state cannot be smaller than zero. In fact,  $\text{tr}(\overline{W}\rho_{BE}) = 0$ . The expectation value for the identity part gives  $-\varepsilon$ . The smallest possible expectation value of the witness  $W$  is achieved by the GHZ state  $|GHZ\rangle = \frac{1}{\sqrt{2}}(|000\rangle + |111\rangle)$ , because this is the eigenvector corresponding to the negative eigenvalue of the witness ( $\lambda = -\frac{3a}{1+a^2} - \varepsilon \approx -1.03$ ). Therefore, the minimal expectation value for a bound entangled state is only about 1/10 of the minimal expectation value for a free entangled state. This is one of the reasons why the detection of bound entanglement is experimentally much more challenging than the detection of free entanglement.

In current liquid NMR experiments a huge ensemble of about  $\sim 10^{19}$  copies of the quantum processors are used. The ensemble in thermal equilibrium follows the Boltzmann distribution dominated by the spin interaction with the external magnetic field. The equilibrium density operator is well approximated by

$$\rho_{eq} = \frac{1}{d} \left( \mathbb{1} + \sum_i \kappa_i I_{zi} \right), \quad (5)$$

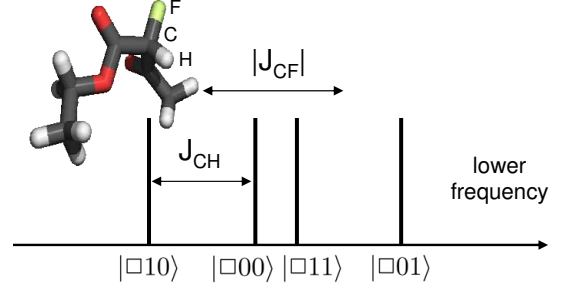


FIG. 1: Schematic carbon NMR spectrum of the CHF group of ethyl 2-fluoroacetate and the stick representation of the molecule. The  $J$ -coupling between the spins as well as the H,F spin states in the computational basis are presented. We use the spin state representation of the form  $|C, H, F\rangle$ , i.e. C (H,F) corresponds to the first (second, third) qubit, respectively. The order of the numbering of the spin states in the spectrum is due to the signs of the  $J$ -coupling constants.

where  $\kappa_i$  is a spin and system specific constant given by  $\kappa_i = \frac{\hbar B_0 \gamma_i}{kT}$  with  $\gamma_i$  being the gyromagnetic ratio.  $I_{zi}$  denotes the  $z$ -component of the angular momentum operator of the  $i$ -th nuclear spin and  $d$  is the dimension of the total system. In usual liquid NMR experiments with a magnetic field of  $\sim 12$  T and protons at ambient temperatures ( $T = 290$  K) we have  $\kappa_H \approx 8.4 \cdot 10^{-5}$ .

The state of interest in our case is given by eq. (1), where we want to generate a specific pseudo bound entangled state  $\rho$ , i.e. the deviation from the normalized identity, with the probability  $p$  available in our system. Our 3-qubit system can reach under the above conditions a fraction of  $p$  for the bound entangled state on the order of  $\kappa$ . To characterize the properties of  $\rho_{BE}$  we will do state tomography to reconstruct the experimentally generated state  $\rho_{exp}$ . Then we will prove entanglement of the part  $\rho_{exp, BE}$ . For this purpose we adopt the usual witness formalism to the pseudo state case, i.e. we shift the witness in eq. (3) by the contribution which comes from the identity, namely we introduce the “pseudo witness”

$$W_{NMR} = \frac{W - \frac{(1-p)}{d} \mathbb{1}}{p}, \quad (6)$$

such that  $\text{tr}(W_{NMR}\rho) = \text{tr}(W\rho_{BE})$ .

We use the heteronuclear 3-qubit system ethyl 2-fluoroacetate [27], consisting of a hydrogen, a carbon and a fluorine spin (see fig. 1) with gyromagnetic ratios of  $\gamma_H \approx 26.75 \cdot 10^7 T^{-1} s^{-1}$ ,  $\gamma_C \approx 6.73 \cdot 10^7 T^{-1} s^{-1}$ ,  $\gamma_F \approx 25.18 \cdot 10^7 T^{-1} s^{-1}$ .

Using such a heteronuclear system has several advantages, first we can apply fast local (spin specific) unitary operations, because of the large Zeeman energy difference between the spins, and second we can focus on the zero order coupling Hamiltonian in the rotating frame representation,  $H = J_{12}I_{z1}I_{z2} + J_{13}I_{z1}I_{z3} + J_{23}I_{z2}I_{z3}$ . Here,  $J_{12} = 161.3$  Hz,  $J_{13} = -190.2$  Hz and  $J_{23} = 47.0$  Hz are the  $J$ -coupling constants between the spins.

We structure the experiment into three parts:

- (i) Generation of a suitable basis state population.
- (ii) Unitary transformations (quantum gates) are applied to the diagonal state to generate  $\rho_{\text{BE}}$ .
- (iii) The generated state is characterized by state tomography and witnesses.

In the first part of the experiment we generate a specific diagonal state, i.e.

$$\rho_d = \frac{1}{8} + \frac{p}{8} (d_a I_{z1} + d_b I_{z2} + d_b I_{z3} + d_c I_{z1} I_{z2} + d_c I_{z1} I_{z3} + d_d I_{z2} I_{z3} + d_e I_{z1} I_{z2} I_{z3}) \quad (7)$$

with the coefficients  $d_a = \frac{2((a-2)a-1)}{a(3a+2)+3} \approx -0.78$ ,  $d_b = -\frac{2(a+1)^2}{a(3a+2)+3} \approx -0.21$ ,  $d_c = 2d_a$ ,  $d_d = 2d_b$  and  $d_e = \frac{48}{a(3a+2)+3} - 8 \approx 3.85$ . We scaled the traceless spin operators in such a way that the scaling factor  $p$  of this deviation density operator corresponds to the probability of our pseudo bound entangled state of eq. (1).

Five experiments are performed to generate different basis state populations. The five diagonal states have the form

$$\begin{aligned} \rho_1 &= \frac{1}{8} + \frac{\kappa_H}{8} (3.77 I_{z1} I_{z2} I_{z3}) \\ \rho_2 &= \frac{1}{8} + \frac{\kappa_H}{8} (-2 I_{z1} I_{z2}) \\ \rho_3 &= \frac{1}{8} + \frac{\kappa_H}{8} (-1.88 I_{z1} I_{z3}) \\ \rho_4 &= \frac{1}{8} + \frac{\kappa_H}{8} (-2 I_{z2} I_{z3}) \\ \rho_5 &= \frac{1}{8} + \frac{\kappa_H}{8} (-I_{z1} - 0.27 I_{z2} - 0.27 I_{z3}). \end{aligned} \quad (8)$$

The manipulation of the equilibrium states to generate each of these states is done by standard hard spin selective pulses,  $j$ -coupling evolution [3] and at the end  $z$ -gradients to destroy the unwanted  $x, y$  magnetization terms, i.e. we apply spatial averaging [28].

The states of these experiments are added with appropriate probabilities to achieve our diagonal density operator  $\rho_d$  in eq. (7) (temporal averaging [29, 30]), i.e.

$$\rho_d = \sum_i q_i \rho_i \quad \text{with} \quad \sum_i q_i = 1 \quad (9)$$

$q_1 \approx 0.36, q_2 = q_5 \approx 0.27, q_3 \approx 0.29, q_4 \approx 0.08$ .

It follows  $p \approx \frac{\kappa_H}{3.61}$ .

On the initial state in eq. (9) we apply a set of unitary transformations to produce the pseudo bound entangled state  $\rho_{\text{BE}}$ . In detail we first apply an effectively line selective  $-\frac{\pi}{2}$ -rotation around the  $y$ -axis in the space  $|000\rangle, |100\rangle$  without affecting the remaining basis states. In the following set of hard rf-pulses and  $j$ -coupling evolutions two gates similar to controlled-NOT gates (with

qubit 1 as control, qubit 2 as target and qubit 3 as target, respectively) are applied [21]. The total unitary transformation of these quantum gates is

$$\begin{aligned} U &= \frac{1}{\sqrt{2}} (|000\rangle\langle 000| + |000\rangle\langle 100| - |111\rangle\langle 000| + |111\rangle\langle 100|) \\ &\quad + i|001\rangle\langle 001| - i|010\rangle\langle 010| + |011\rangle\langle 011| \\ &\quad + |100\rangle\langle 111| + i|101\rangle\langle 110| - i|110\rangle\langle 101|. \end{aligned} \quad (10)$$

The generated state is characterized by state tomography in the usual NMR setting [29], i.e. before the detection the spin selective rotations  $Y_1 E_2 E_3$ ,  $E_1 E_2 Y_3$ ,  $E_1 E_2 X_3$ ,  $Y_1 Y_2 E_3$ ,  $E_1 X_2 X_3$ ,  $Y_1 Y_2 Y_3$  and  $X_1 X_2 X_3$  are performed. Here  $X_i$  ( $Y_i$ ) denotes a  $\pi/2$  rotation of the  $i$ -th spin about the  $x$ - ( $y$ -) axis and  $E_i$  is the identity operation. In the experiments only the carbon spin (see fig. 1) is detected. To get the information of the H (F) spins an appropriate swap gate to the carbon and H (F) spin is performed before detection. The experimental data gained by this procedure leads to an overdetermined set of linear equations for reconstructing the density matrix. We reconstruct the density operator from the experimental data by a least squares fit [32].

The experimentally generated state is shown in Fig. 2. The excellent agreement between ideal and generated state reflects the high controllability as well as low decoherence of our NMR system. The main deviations are due to partial relaxation and pulse imperfections during the experiment [41].

The fraction  $p$  of the pseudo bound entangled state in  $\rho_{\text{exp}} = \frac{(1-p)}{8} \mathbb{1} + p \rho_{\text{BE}}$  is in our case about  $p \approx 10^{-5}$ .

How close this state is in comparison to the ideal one can be expressed in terms of the overlap or the distance between real and ideal state. We find a high Uhlmann fidelity [33] for the pseudo bound entangled state, namely

$$F_u = \text{tr} \left( \sqrt{\sqrt{\rho_{\text{BE,theo}}} \rho_{\text{BE,exp}} \sqrt{\rho_{\text{BE,theo}}}} \right) = 0.98, \quad (11)$$

and a small trace distance [34],

$$d_t = \frac{\text{tr} \left( \sqrt{X^\dagger X} \right)}{2} = 0.09, \quad \text{with} \quad X = \rho_{\text{BE,theo}} - \rho_{\text{BE,exp}}. \quad (12)$$

The standard deviation of the density operator elements are obtained from the least square method. They are used to calculate the standard deviation of the witness expectation value by error propagation. This deviation accounts for the inconsistencies in the overhead of the experimental data, which are due to imperfections in the tomography procedure. The reconstructed state  $\rho_{\text{BE,exp}}$  has a positive partial transpose with respect to any bipartite splitting. The witness expectation value of the experimental state is

$$\text{tr}(W \rho_{\text{BE,exp}}) = -0.029 \pm 0.010, \quad (13)$$

i.e. the state is bound entangled. The ideal expectation value would have been  $-0.11$ . Remember that the witness expectation value can vary from  $-1.0$  to  $+1.8$ , i.e.

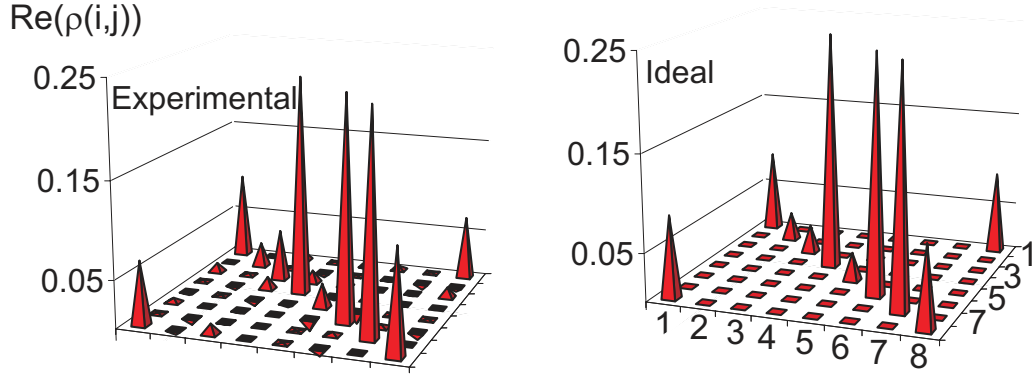


FIG. 2: Experimental and ideal real matrix elements of  $\rho_{BE}$ . All imaginary elements of the experimental state are small ( $< 0.019$ ).

the possible range  $-0.11 \leq \langle W \rangle < 0$  for bound entanglement is rather small - thus, already small deviations from the ideal situation can have large effects.

In conclusion, we have generated and detected pseudo bound entanglement with an NMR experiment. We reached a high fidelity,  $F = 0.98$ , of the created state with respect to the ideal one. The partial transpositions of the state were shown to be positive with respect to any bipartite splitting. The pseudo witness that we used had a negative expectation value, thus proving that the state was indeed entangled. Here we calculated the expectation value of the witness operator using the reconstructed

state. This is more appropriate than to detect the witness directly [39], because some experimental errors are “averaged” during the least square method used in the state tomography procedure. - Thus, we have shown that bound entanglement can exist in the laboratory.

After completion of this manuscript we learned about related work by Amselem *et al.* [40].

We thank Otfried Gühne and Matthias Kleinmann for enlightening discussions. We acknowledge financial support from the EU Integrated projects SCALA and SEC-OQC, as well as from Deutsche Forschungsgemeinschaft (DFG).

- 
- [1] E. Schrödinger, *Naturwissenschaften* **23**, 807 (1935).
  - [2] D. Bruß and G. Leuchs, *Lectures on Quantum Information* (Wiley-VCH, 2007).
  - [3] J. Stolze and D. Suter, *Quantum Computing: A Short Course from Theory to Experiment* (Wiley-VCH, 2004).
  - [4] R. Horodecki, P. Horodecki, M. Horodecki, and K. Horodecki, arXiv: quant-ph/0702225 (2007).
  - [5] O. Gühne and G. Tóth, arXiv:0811.2803 (2008).
  - [6] A. Aspect, P. Grangier, and G. Roger, *Phys. Rev. Lett.* **47**, 460 (1981).
  - [7] Q. Turchette, C. Wood, B. King, C. Myatt, D. Leibfried, W. Itano, C. Monroe, and D. Wineland, *Phys. Rev. Lett.* **81**, 3631 (1998).
  - [8] D. Bouwmeester, J. Pan, M. Daniell, H. Weinfurter, and A. Zeilinger, *Phys. Rev. Lett.* **82**, 1345 (1999).
  - [9] D. Leibfried, M. Barrett, T. Schaetz, J. Britton, J. Chiaverini, W. Itano, J. Jost, C. Langer, and D. Wineland, *Science* **304**, 1476 (2004).
  - [10] C. Roos, M. Riebe, H. Häffner, W. Hänsel, J. Benhelm, G. Lancaster, C. Becher, F. Schmidt-Kaler, and R. Blatt, *Science* **304**, 1478 (2004).
  - [11] M. Bourennane, M. Eibl, C. Kurtsiefer, S. Gaertner, H. Weinfurter, O. Gühne, P. Hyllus, D. Bruß, M. Lewenstein, and A. Sanpera, *Phys. Rev. Lett.* **92**, 087902 (2004).
  - [12] C. Lu, X. Zhou, O. Gühne, W. Gao, J. Zhang, Z. Yuan, A. Goebel, T. Yang, and J. Pan, *Nature Phys.* **3** (2007).
  - [13] H. Häffner, W. Hänsel, C. Roos, J. Benhelm, D. Chek-al-kar, M. Chwalla, T. Körber, U. Rapol, M. Riebe, P. Schmidt, C. Becher, O. Gühne, W. Dür, R. Blatt, *Nature* **438**, 643 (2005).
  - [14] D. Leibfried, E. Knill, S. Seidelin, J. Britton, R. Blakestad, J. Chiaverini, D. Hume, W. Itano, J. Jost, C. Langer, et al., *Nature* **438**, 639 (2005).
  - [15] M. Horodecki, P. Horodecki, and R. Horodecki, *Phys. Rev. Lett.* **80**, 5239 (1998).
  - [16] K. Horodecki, M. Horodecki, R. Horodecki, and J. Oppenheim, *Phys. Rev. Lett.* **94**, 160502 (2005).
  - [17] G. Tóth, C. Knapp, O. Gühne, and H. Briegel, *Phys. Rev. Lett.* **99**, 250405 (2007).
  - [18] H. Kampermann, Talk at DPG meeting, Darmstadt (2008); Talk at SCALA conference, “International Conference on Scalable Quantum Computing with Light and Atoms”, Cortina (2009).
  - [19] A. Acin, D. Bruß, M. Lewenstein, and A. Sanpera, *Phys. Rev. Lett.* **87**, 040401 (2001).
  - [20] P. Hyllus, M. Alves, D. Bruß, and C. Macchiavello, *Phys. Rev. A* **70**, 032316 (2004).
  - [21] R. Laflamme, E. Knill, W. Zurek, P. Catasti, and S. Mariappan, *Philos. T. Roy. Soc. A* **356**, 1941 (1998).
  - [22] J. A. Jones, M. Mosca, and R. H. Hansen, *Nature* **393**, 344 (1998).

- [23] H. K. Cummins, C. Jones, A. Furze et al, Phys. Rev. Lett. **88**, 187901 (2002).
- [24] D. Suter, and T.S. Mahesh, J. chem. Phys. **128**, 052206 (2008).
- [25] C.A. Ryan, C. Negrevergne, M. Laforest, E. Knill, R. Laflamme, Phys. Rev. A **78**, 012328 (2008).
- [26] L.M.K. Vandersypen, and I.L. Chuang, Rev. Mod. Phys. **76**, 1037 (2004).
- [27] J. Zhang, N. Rajendran, X. Peng, and D. Suter, Phys. Rev. A **76**, 012317 (2007).
- [28] D. Cory, M. Price, and T. Havel, Physica D **120**, 82 (1998).
- [29] I.L. Chuang, N. Gershenfeld, M. Kubinec, and D. Leung, Proc. R. Soc. Lond. A **454**, 447 (1998).
- [30] L.M.K. Vandersypen, M. Steffen, G. Breyta, C.S. Yannoni, R. Cleve, and I.L. Chuang, Phys. Rev. Lett. **85**, 5452 (2000).
- [31] N. Gershenfeld and I. Chuang, Science **275**, 350 (1997).
- [32] G. Long, H. Yan, and Y. Sun, J. Opt. B-Quantum S. O. **3**, 376 (2001).
- [33] A. Uhlmann, Rep. Math. Phys. **9**, 273 (1976).
- [34] M. Nielsen and I. Chuang, *Quantum Computation and Quantum Information* (Cambridge University Press, 2000); D. Bruß and G. Leuchs (Eds.), *Lectures on Quantum Information* (Wiley-VCH, 2007).
- [35] L. Gurvits and H. Barnum, Phys. Rev. A p. 032322 (2005).
- [36] A. Datta and G. Vidal, Phys. Rev. A **75**, 042310 (2007).
- [37] Z. Hradil, J. Řeháček, J. Fiurášek, and M. Ježek, Lect. Notes Phys. **649**, 59 (2004).
- [38] R. Blume-Kohout, arXiv:quant-ph/0611080 (2006).
- [39] O. Gühne, P. Hyllus, D. Bruß, A. Ekert, M. Lewenstein, C. Macchiavello, and A. Sanpera, Phys. Rev. A **66**, 062305 (2002).  
OpticBoundEnt
- [40] E. Amselem and M. Bourennane, Nat. Phys., doi:10.1038/nphys1372 (2009).
- [41] We want to note here that in the NMR weak measurement scheme the usual statistical errors due to limited number of individual measurements play no role. I.e. it is not necessary to consider reconstruction schemes using maximum likelihood [37] or Bayesian mean estimation [38].